Particle dynamics in a viscously decaying cat's eye: The effect of finite Schmidt numbers

P. K. Newton
Department of Mathematics, University of Illinois, Urbana, Illinois 61801

Eckart Meiburg
Department of Aerospace Engineering, University of Southern California, Los Angeles, California 90089

(Received 10 September 1990; accepted 18 December 1990)

The dynamics and mixing of passive marker particles for the model problem of a decaying cat's eye flow is studied. The flow field corresponds to Stuart's one-parameter family of solutions [J. Fluid Mech. **29**, 417 (1967)]. It is time dependent as a result of viscosity, which is modeled by allowing the free parameter to depend on time according to the self-similar solution of the Navier–Stokes equations for an isolated point vortex. Particle diffusion is numerically simulated by a random walk model. While earlier work had shown that, for small values of time over Reynolds number $t/\mathrm{Re} \ll 1$, the interval length characterizing the formation of lobes of fluid escaping from the cat's eye scales as $\mathrm{Re}^{-1/2}$, the present study shows that, for the case of diffusive effects and $t/\mathrm{Pe} \ll 1$, the scaling follows $\mathrm{Pe}^{-1/4}$. A simple argument, taking into account streamline convergence and divergence in different parts of the flow field, explains the $\mathrm{Pe}^{-1/4}$ scaling.

I. INTRODUCTION

The analysis of mixing and stirring processes in two- and three-dimensional flows recently has received increased attention. In particular, a variety of temporally and spatially periodic flow fields have been analyzed with the help of tools provided by the theory of dynamical systems. A key finding has been that many smooth velocity fields give rise to extremely complicated particle trajectories, thus resulting in what has become known as chaotic advection or Lagrangian turbulence. For a review of many interesting examples, see Ottino.[1] While the theory of dynamical systems is most powerful for analyzing flows with some periodicity, our focus in the present paper will be on particle dynamics and mixing processes in two-dimensional unsteady but temporally nonperiodic flows, for which traditional tools such as Poincare sections are of limited help. Hence we have to resort to other analytical and numerical calculations to quantify the mixing process.

In particular, we will, in the present study, continue our earlier investigation of a viscously decaying row of point vortices (Meiburg and Newton[2]). This flow displays enhanced mixing without giving rise to chaotic streamlines. While our earlier work focused on the case of small values of time over Reynolds number t/Re and infinite Schmidt numbers, i.e., nondiffusing particles, we now aim at evaluating the effect of particle diffusion, thus introducing a further dimensionless quantity in the form of the Peclet number Pe. The model flow on which we base our investigation employs the one-parameter family of solutions to the Euler equations known as Stuart vortices (Stuart[3] and Pierrehumbert and Widnall[4]). A detailed description of how we account for viscosity is given in Meiburg and Newton,[2] and we will review the key features in Sec. II. In Sec. III A, we will present some scaling results for the case of diffusing particles in inviscid flow, while III B will consider the situation in which both Reynolds number and Peclet number are finite. Finally, Sec. IV will summarize the results and draw some conclusions.

II. MODEL FLOW

The model flow that we are investigating is based on the one-parameter family of solutions to the steady Euler equations known as the Stuart vortices:

$$\psi(x,y) = \ln[\cosh(2\pi y) - \rho \cos(2\pi x)],$$

where ψ is the dimensionless streamfunction. The parameter ρ determines the concentration of vorticity. In particular, for $\rho = 1$ we obtain a periodic row of point vortices, whereas $\rho = 0$ corresponds to a parallel shear flow with a hyperbolic tangent velocity profile. The key feature of our approach to modeling a viscously decaying row of point vortices is the assumption that, for small values of t/Re, each point vortex will diffuse in a fashion similar to a single isolated point vortex, for which the exact solution to the Navier–Stokes equations is known. Specifically, we assume that the core size of the diffusing vortices grows proportionally to $(t/\mathrm{Re})^{1/2}$. As explained in detail in our earlier work, this approach leads to a time-dependent value of the parameter ρ of the form

$$\rho(t) = 1/[\cosh(4\pi\sqrt{t/\mathrm{Re}})].$$

Here, the Reynolds number $\mathrm{Re} = \Gamma/\nu$, with Γ being the circulation of an individual vortex and ν representing the kinematic viscosity of the fluid. While we note that this model flow does not represent an exact solution to the Navier–Stokes equations, it captures the basic effect of a vorticity distribution that is smoothed out by viscous diffusion.

An important question that we briefly address here concerns the error introduced by our model. As discussed by Meiburg and Newton,[2] the Stuart streamfunction leads to a vorticity distribution of the form

 0899-8213/91/051068-05$02.00

$$\omega = -(2\pi)^2[1-\rho^2(t)]/[\cosh(2\pi y)-\rho(t)\cos(2\pi x)].$$

If we substitute this expression into the full time-dependent vorticity form of the Navier–Stokes equations, the nonlinear terms are satisfied identically, and we are left with the linear terms

$$E(x,y,t) = -[\omega_t - (1/\mathrm{Re})\,\nabla^2\omega].$$

Plots of $E(x,y,t)$ are shown in Fig. 1 for increasing times and $\mathrm{Re} = 10^3$. It is evident from Fig. 1(a) that, at $t = 0.1$, the error is localized around the center and dies off rapidly away from it. Note the very singular behavior directly at the center where we observe a sharp spike. The main point of relevance to our results is that the error is smallest in the region of the separatrices, so that our results should be valid at least for short times. As time increases, the error spreads away from the center and pollutes the entire flow field.

In summary, as a result of viscous diffusion, the flow field becomes time dependent and the width of the cat's eyes decreases. Thus viscosity causes the trapped fluid to leak out of the cat's eye. A particle that is initially trapped within the cat's eye will cross the separatrix at some finite time after performing a number of orbits around the vortex core that depends on the initial particle location. Hence we can identify an infinite number of alternating layers of length l_1, l_2, etc., along the x axis within the cat's eye that become infinitesimally thin near the vortex center (Fig. 2). These layers characterize initial data according to whether a particle will escape above the mixing layer and continue moving right, or below the mixing layer and continue moving left. The process of crossing the separatrix is the essential mechanism that leads to sensitive behavior and enhanced mixing. In our earlier work (Meiburg and Newton[2]), we showed that the lengths of these intervals scale with $\mathrm{Re}^{-1/2}$.

If we also allow for the diffusion of particles, an additional dimensionless parameter arises in the form of the Peclet number $\mathrm{Pe} = \Gamma/D$, where D is the diffusion coefficient. The Schmidt number Sc denotes the ratio of kinematic viscosity and diffusion coefficient $\mathrm{Sc} = \mathrm{Pe}/\mathrm{Re} = \nu/D$. The diffusive length scale introduced into the problem by D lets particles escape from the cat's eye, even in the case of inviscid steady flow, simply by diffusion across the separatrix. In analogy to the above intervals that characterize where nondiffusing particles escape from the cat's eye in the viscous case, we can now define intervals of the size d_1, d_2, etc., for the case of diffusing particles in inviscid flow in the following way: If we release diffusing particles at a fixed location along the x axis, and more than a certain fraction, e.g., 10%, es-

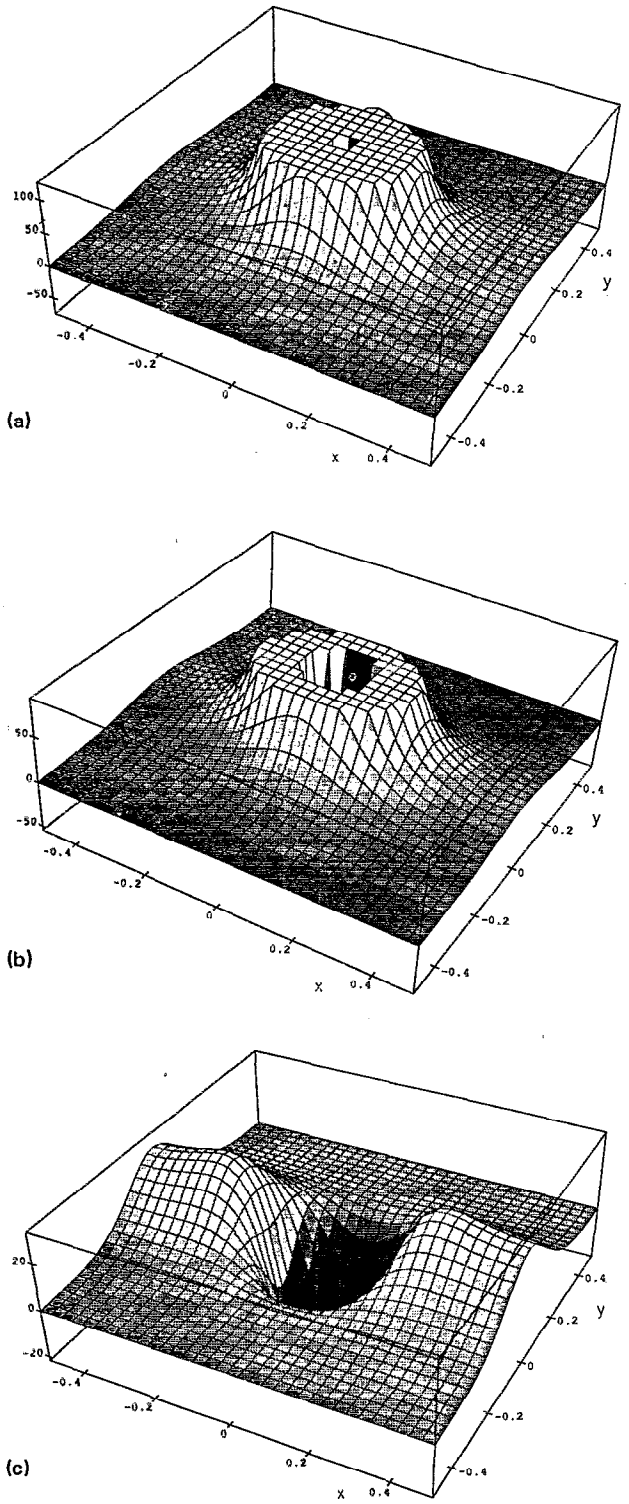

FIG. 1. The error of the model flow with respect to the full Navier–Stokes equations at times $t = 0.1$, 1, and 10; $\mathrm{Re} = 10^3$. Notice that, especially at small times, the error is essentially limited to the region near the vortex core.

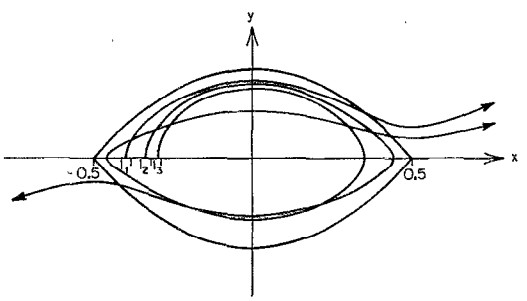

FIG. 2. The shrinking of the cat's eye results in lobes of fluid leaking out of the trapped region. Fluid particles initially distributed along intervals on the x axis are associated with the lobes. The interval lengths scale with $\mathrm{Re}^{-1/2}$.

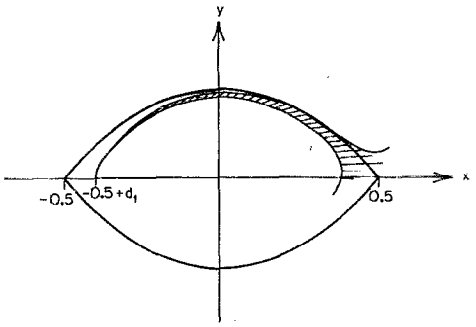

FIG. 3. In the case of inviscid flow, fluid particles can escape the trapped region as a result of mass diffusion. In analogy to the viscous case without mass diffusion, we can define intervals d_1, d_2, etc., according to how often the particles initially distributed along the interval circle the vortex before a certain fraction of them escapes.

capes during the first half-cycle, then the point of release belongs to interval d_1 (Fig. 3). The border of d_1 is reached at the point for which exactly 10% of the released particles escape during the first half-cycle. Then, d_2 extends from this location to the point that leads to 10% of the particles escaping over the first two half-cycles, etc. Also, d_3 and further intervals are defined correspondingly. In the following, we aim at finding the scaling laws for these intervals. We will present both numerical simulations and analytical scaling calculations. The inviscid case will be considered in Sec. III A, whereas we will focus on the viscous case with particle diffusion (for which intervals can be defined correspondingly) in Sec. III B.

III. SCALING RESULTS FOR THE INTERVAL SIZES

A. Diffusing particles in inviscid flow

Figure 4 shows numerical results for d_1 as a function of Pe. The computations employed 1000 particles released simultaneously on the x axis near the left stagnation point. We iterated to find the release location $-0.5+d_1$ that led to the escape of 10% of the particles during the first half-cycle. The particle motion was calculated by superimposing a random walk component on the motion calculated from the streamfunction (1) as follows:

$$\frac{dx}{dt}=\frac{2\pi\sinh(2\pi y)}{\cosh(2\pi y)-\rho(t)\cos(2\pi x)},$$

$$\frac{dy}{dt}=\frac{-2\pi\rho(t)\sin(2\pi x)}{\cosh(2\pi y)-\rho(t)\cos(2\pi x)}.$$

The modeling of particle diffusion by a random walk component is a standard technique and has been employed by several authors, e.g., Aref and Jones.[5] Briefly, at the end of every time step Δt, the random walk components in the x and y directions are found by means of random numbers from a Gaussian distribution with variance $2\Delta t/\mathrm{Pe}$. The particle motion due to the underlying velocity field is computed by means of a fourth-order Runge–Kutta scheme. Figure 5 shows the evolution of a typical patch of particles at different times. From Fig. 4, we recognize that, for small values of t/Pe, d_1 scales with $\mathrm{Pe}^{-1/4}$. It might be considered surprising that the interval size in the viscous flow without particle diffusion scales as $\mathrm{Re}^{-1/2}$, whereas for the inviscid flow with particle diffusion we find $\mathrm{Pe}^{-1/4}$. As both dimensionless parameters describe the effect of a diffusion process—viscous diffusion and particle diffusion, respectively—one might expect the dependence on Re and Pe to be the same. In the following, we will show how the $\mathrm{Pe}^{-1/4}$ scaling arises as a result of the interaction between particle diffusion and converging and diverging streamlines of the underlying inviscid velocity field.

The particles released near the left stagnation point are initially located in a region of small velocity. As they leave the stagnation point area, they speed up and eventually reach their maximum velocity around $x=0$, where the cat's eye is widest. Consequently, from their release time to when they reach their maximum y location, the particles spend most of the time near the left stagnation point. Furthermore, this is also the region in which the diffusion across streamlines is most pronounced, as the concentration gradients are very high initially. Hence most of the diffusive component of the particle motion takes place in this area. For the purpose of finding the proper scaling, we can idealize the time interval t_a from the release time to when the particles reach their maximum y location by assuming that the particles spend the whole time t_a diffusing from their point of release, upon which they are instantaneously transported along streamlines to $x=0$. If we denote by f_1 the square root of the variance of the particle distribution function near the release

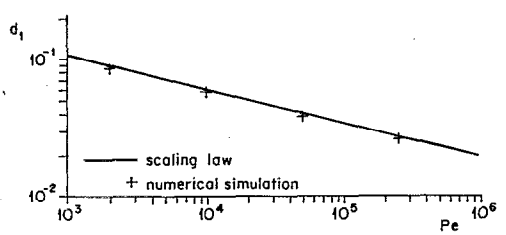

FIG. 4. Inviscid flow: The interval size d_1 scales with $\mathrm{Pe}^{-1/4}$.

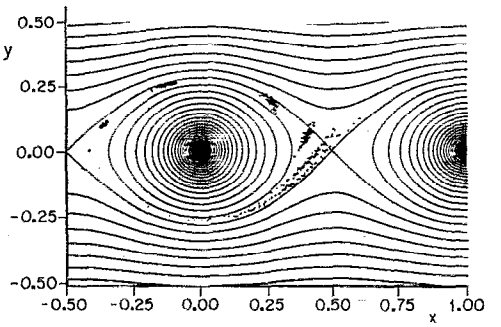

FIG. 5. Example of particles escaping due to diffusive effects in inviscid flow. The patch of particles released near the left corner of the cat's eye is shown for various successive times.

point after t_a, we find that f_1 is proportional to $(t_a/\mathrm{Pe})^{1/2}$. However, we showed in Meiburg and Newton[2] that streamlines separated by ε near the stagnation point are only separated by ε^2 at $x=0$. As a result, we expect the width f_1 of the particle distribution function to be t_a/Pe by the time the particles reach $x=0$. As the mapping $\varepsilon \to \varepsilon^2$ only holds for $\varepsilon \ll 1$, the above argument is restricted to small values of t/Pe, i.e., to particle distributions with a narrow half-width. Under these circumstances, concentration gradients are much stronger normal to the streamlines than along them, and as a result we can, to the leading order, neglect concentration gradients in the direction of the streamlines and assume a Gaussian distribution in the normal direction. It follows that the particle distribution function at $x=0$ and at time t_a is steeper and narrower than that of a patch of particles diffusing for a time t_a but otherwise at rest, which would have a width of $(t_a/\mathrm{Pe})^{1/2}$. Consequently, we can assign the actual particle distribution function at $x=0$ and at time t_a a "hypothetical age" t_{hyp}, which can be calculated from $t_a/\mathrm{Pe} = (t_{\mathrm{hyp}}/\mathrm{Pe})^{1/2}$. We then get $t_{\mathrm{hyp}}/t_a = t_a/\mathrm{Pe} \ll 1$.

We now have to determine the evolution of the width of the particle distribution function as the particle patch moves from $x=0$ to the region near the right stagnation point. This evolution is dominated by the initial diffusion of the particles in the area near $x=0$, as the streamlines are close to each other here and the concentration gradients are still large. The width is subsequently increased by the divergence of the streamlines near the right stagnation point. Again, we can idealize the situation by assuming the particles to diffuse near $x=0$ during the interval $t_a < t < 2t_a$, upon which they are instantaneously convected along streamlines toward the right stagnation point. We find for the square root of the variance f_1' at $t=2t_a$ near $x=0$

$$f_1' \sim [(t_a + t_{\mathrm{hyp}})/\mathrm{Pe}]^{1/2}.$$

With $t_{\mathrm{hyp}} \ll t_a$, this simplifies to

$$f_1' \sim (t_a/\mathrm{Pe})^{1/2}.$$

This simplification reflects the fact that, in the early stages of the particle distribution function's evolution, i.e., until the particles reach $x=0$, the diffusion of the particles is partially compensated by the convergence of the streamlines, which keeps the particle distribution function steep. As a result, the particle distribution function at later stages to the leading order scales in the same way as if the particles were released at $x=0$. Bearing in mind that streamlines ε^2 apart near $x=0$ are separated by ε near the right stagnation point, we obtain for the square root of the variance f_2 of the particle patch near the right stagnation point

$$f_2 = (f_1')^{1/2} \sim (t_a/\mathrm{Pe})^{1/4}$$

so that

$$f_2 \sim \mathrm{Pe}^{-1/4}.$$

The above result is in contrast to the square root of the variance of a diffusing particle patch otherwise at rest or convected along parallel streamlines, which would have acquired a width of $O(\mathrm{Pe}^{-1/2})$ after the same time. It remains to be shown that d_1 exhibits the same scaling as f_2. This can easily be understood from the following argument: Near the right stagnation point, the distribution function of particles released at $-0.5+d_1$ has the width f_2. For small values of t/Pe, this width is much smaller than the radius of curvature of the streamlines, and consequently the particle distribution function near the right stagnation point can be considered as a Gaussian distribution centered approximately around $0.5-d_1$. Above, we had defined d_1 in such a way that $-0.5+d_1$ marks the location for which a fixed fraction of the released particles escape, i.e., are located to the right of the right stagnation point. This means that, for different Pe,

$$\frac{\int_{x=0.5}^{\infty} e^{-(x-0.5+d_1)^2/f_2^2}\,dx}{\int_{-\infty}^{\infty} e^{-(x-0.5+d_1)^2/f_2^2}\,dx} = \text{const.}$$

Transforming

$$x' = (x-0.5+d_1)/f_2,$$

we obtain

$$\frac{\int_{x'=d_1/f_2}^{\infty} e^{-x'^2}\,dx'}{\int_{-\infty}^{\infty} e^{-x'^2}\,dx'} = \text{const.}$$

This is possible only if the integral boundary does not depend on Pe, i.e., if d_1 and f_2 depend on Pe in the same fashion. It follows that d_1 has to scale in the same way as f_2, so that

$$d_1 \sim \mathrm{Pe}^{-1/4},$$

as observed in the numerical simulation.

In summary, the scaling of the particle distribution function near the right stagnation point is determined by two effects: first, by simple diffusion of the particles, and second, by the divergence of the streamlines between $x=0$ and the area close to the right stagnation point. Diffusion alone would imply a scaling with $\mathrm{Pe}^{-1/2}$, however, the $\varepsilon^2 \to \varepsilon$ mapping leads to $\mathrm{Pe}^{-1/4}$. The evolution of the particle distribution function as a result of diffusion as well as streamline convergence and divergence in the different parts of the flow field is sketched in Fig. 6. It shows how particle diffusion in a periodic flow field of converging and diverging streamlines

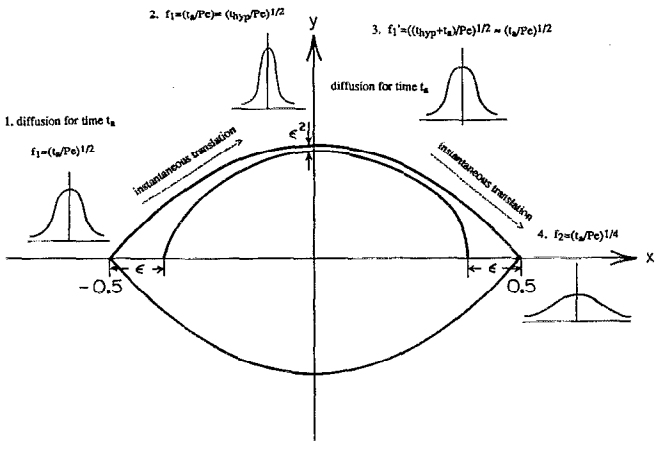

FIG. 6. Schematic diagram of the evolution of the particle distribution function under the combined effects of particle diffusion and convection in a field of converging and diverging streamlines.

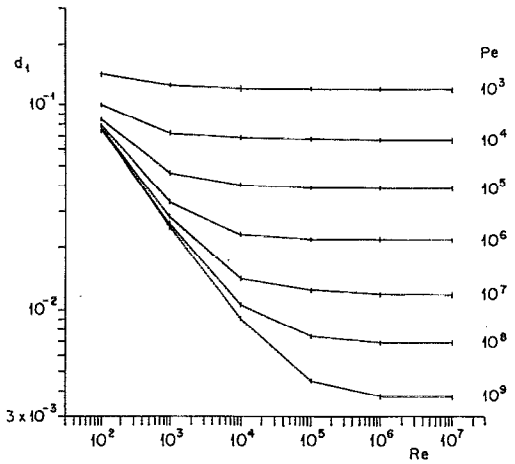

FIG. 7. Diffusing particles in viscous flow: d_1 (Re) for various constant values of Pe. If $\mathrm{Pe} \gg \mathrm{Re}^2$, d_1 only depends on Re as $\mathrm{Re}^{-1/2}$. For $\mathrm{Pe} \ll \mathrm{Re}^2$, d_1 only depends on Pe as $\mathrm{Pe}^{-1/4}$.

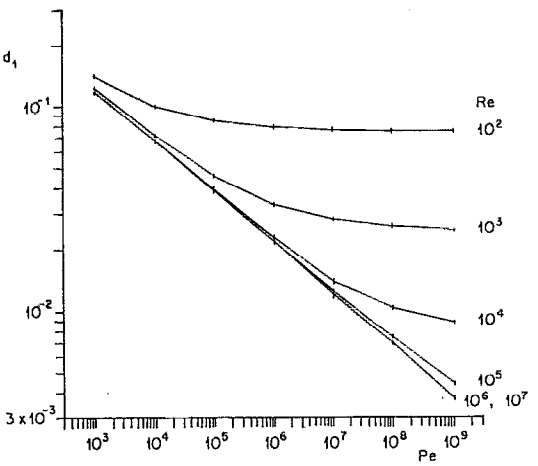

FIG. 8. Diffusing particles in viscous flow: d_1 (Pe) for various constant values of Re. If $\mathrm{Re}^2 \gg \mathrm{Pe}$, d_1 only depends on Pe as $\mathrm{Pe}^{-1/4}$. For $\mathrm{Re}^2 \ll \mathrm{Pe}$, d_1 only depends on Re as $\mathrm{Re}^{-1/2}$.

can lead to dramatically different final concentration profiles.

B. Diffusing particles in viscous flow

We now consider the case of diffusing particles in a viscously decaying row of vortices. As before, the escape of 10% of the particles defines the borders between intervals. Figure 7 shows the dependence of d_1 on the Reynolds number for various values of Pe. We observe that, as long as $\mathrm{Pe} \gg \mathrm{Re}^2$, Pe is of little influence, and $d_1 \sim \mathrm{Re}^{-1/2}$. However, as Re increases, Pe provides a lower bound for the interval size and d_1 asymptotically approaches this value, which scales with $\mathrm{Pe}^{-1/4}$. Figure 8, which shows d_1 as a function of Pe for various values of Re, can be interpreted in a similar fashion. As long as $\mathrm{Re}^2 \gg \mathrm{Pe}$, Re is of little influence and $d_1 \sim \mathrm{Pe}^{-1/4}$. However, as Pe increases, the Reynolds number provides a lower limit for d_1, which now scales with $\mathrm{Re}^{-1/2}$. We notice that, in general, the size of d_1 decreases with increasing Re and Pe.

IV. SUMMARY AND CONCLUSION

We have studied the dynamics and mixing of particles for the model problem of a decaying cat's eye flow. Viscosity introduces time dependency into the problem and is accounted for by letting the free parameter in Stuart's family of solutions depend on time according to the self-similar solution of the Navier–Stokes equations for an isolated point vortex. Particle diffusion is numerically simulated by a random walk model. While earlier work had shown that, for $t/\mathrm{Re} \ll 1$, the interval length characterizing the formation of lobes of fluid escaping from the cat's eye scales as $\mathrm{Re}^{-1/2}$, the present study shows that, for the case of diffusive effects and $t/\mathrm{Pe} \ll 1$, the scaling follows $\mathrm{Pe}^{-1/4}$. While it might appear surprising that the two mechanisms of momentum and mass diffusion lead to different dependencies on Re and Pe, a simple argument that takes into account the convergent and divergent nature of the streamline pattern in different parts of the flow field elucidates the $\mathrm{Pe}^{-1/4}$ scaling.

ACKNOWLEDGMENTS

The authors acknowledge support by the National Science Foundation through Grants No. CTS-9058065 (to EM) and No. NSF DMS 90-00593 (to PKN). The San Diego Supercomputer Center has provided time on its CRAY-Y/MP computer.

[1] J. M. Ottino, *The Kinematics of Mixing: Stretching, Chaos and Transport*, Cambridge Texts in Applied Mathematics (Cambridge U. P., Cambridge, 1989).

[2] E. Meiburg and P. K. Newton, to appear in J. Fluid Mech., 1991.

[3] J. T. Stuart, J. Fluid Mech. **29**, 417 (1967).

[4] R. T. Pierrehumbert and S. E. Widnall, J. Fluid Mech. **102**, 301 (1981).

[5] H. Aref and S. W. Jones, Phys. Fluids A **1**, 470 (1989).